RSC Advances

ROYAL SOCIETY OF CHEMISTRY

www.rsc.org/advances

Cite this: DOI: 10.1039/c0xx00000x

www.rsc.org/xxxxxx

ARTICLE TYPE

Synthesis and Co-assembly of Gold Nanoparticles Functionalized by Pyrene-thiol Derivative

Yongsheng Mi,[a] Pengxia Liang,[a] Zhou Yang,*[a] Dong Wang,*[a] Wanli He,[a] Hui Cao[a] and Huai Yang[b]

Received (in XXX, XXX) Xth XXXXXXXXX 20XX, Accepted Xth XXXXXXXXX 20XX

DOI: 10.1039/b000000x

We successfully synthesized a series of gold nanoparticles capped with 11-(4-(pyren-1-yl)phenoxy)undecane-1-thiol (A-SH) and with 1-dodecanethiol. The homodispersed gold nanoparticles were fully verified by TEM, UV-Vis and PL spectroscopy. TEM images of nanoparticles showed similar particles size at approximately 2.5 nm as well as evidenced by the absorption spectra. By solvent-exchange co-self-assembly of pyrene derivative composited with these functionalized nanoparticles, the different arrangements of Au nanoparticles were observed. Comparing to Au nanoparticles functionalized by 1-dodecanethiol (GNP), the pyrene-thiol-capped gold nanoparticles (GNP-A) showed better dispersity in the pyrene derivative matrix because of their π-π interactions.

Introduction

Metal hybrids of chromophores assembled as two- or three-dimensional assemblies provide routes for hybrid materials with optical, electrical and photochemical properties.[1-7] Most of the earlier studies on the interaction between fluorophores and metals are limited to bulk gold surfaces, functionalized with self-assembled monolayers.[8] For instance, 1D array of gold NPs have potential for the directional transfer of photons and/or electrons, due to a dramatic increase of particle-particle interaction, leading to construction of nanoscale devices,[9] such as plasmon waveguides, magnetic logic, quantum cellular automata, and coulomb blockade devices.[10, 11]

Since the important report by Brust et al. in 1994,[12] extensive chemical and physical studies have been carried out on alkanethiols-capped gold nanoparticles, which are also referred to three-dimensional monolayers protected clusters. These investigations include new approaches to the synthesis of monodispersed gold nanoparticles, preparation of superlattice structures composed of nanoparticles, controllable arrangements of nanoparticles with supramolecular chemistry principle, in-place exchange reaction, and functionalization of nanoparticles.[13] Many groups are interested in the π-π interactions of organic protective agents to control various types of assembly of gold NPs.[14] For example, spherical aggregates by terthiophene[15] and 2D assembly by pyrene units[16] or by thiophene ligands.[17] 1D assembly of gold NPs can also be realized by fixation on the 1D matrix by π-π interactions of the functional groups such as pyrene derivatives.[18]

Unlike other aromatic compounds, pyrene-based molecular systems have proved to be a versatile class of probe molecule in both chemistry and biology.[19] Pyrene and its derivatives, in the monomeric form, show structured absorption and emission peaks, which are extremely sensitive to their environments.[20] Besides, pyrene is known to form an electron donor-acceptor complex with electron-acceptor molecules and already has been incorporated into self-assembled systems owing to the strong π-π interactions.[21] Thus, it would be interesting to prepare gold nanoparticles capped by alkanethiols containing pyrene units and hence employ transmission electron microscopy to study the molecular arrangements of alkanethiol ligands. Indeed, thiols with pyrene units have been incorporated into the self-assembled monolayer structures,[22] but the co-assembly of pyrene-thiol capped Au nanoparticles and pyrene derivatives has been reported rarely.

Here, we presented the synthesis and characterization of a kind of pyrene-thiol-capped gold nanoparticles and corresponding gold nanoparticles capped with 1-dodecanethiol.[12] In particular, we have focused our attention on the self-assembly properties of these nanoparticles composited with pyrene derivative which has well self-assembly behavior. By co-assembly of the organic-metal composites, π-π interactions will be fully exploited and regular morphologies could be observed by TEM.

Results and discussion

Synthesis and TEM characterization

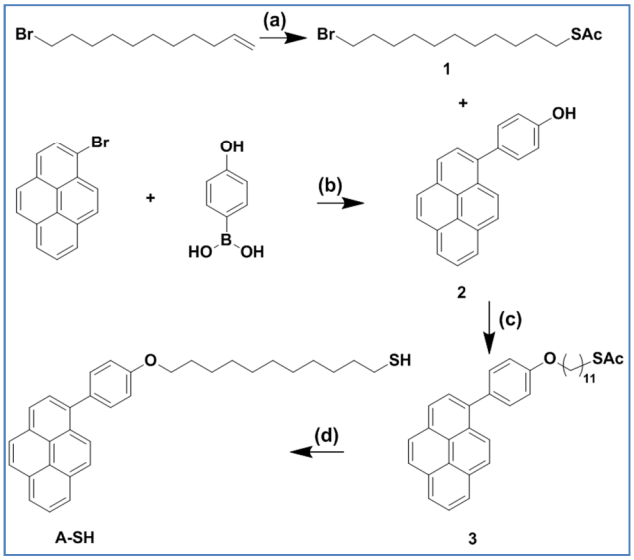

Scheme 1. Molecular structures and synthetic routes of pyrene-thiol based derivatives. (a) AIBN, toluene, 85 °C, 8 h; (b) (4-hydroxyphenyl)boronic acid, $Pd(PPh_3)_4$, THF/TEA, 80 °C, 8 h; (c) K_2CO_3, DMF,24 h; (d) HCl, MeOH, rt, 8 h.

Molecular structure of compound A-SH which had a phenyl pyrene core connected with alkyl-thiol. The pyrene cores could provide well photophysical and self-assembly properties, as well as the alkyl-thiol group could be connected with Au nanoparticles by Au-SH interactions. The introduction of anisole group could reduce the difficulty by typical Suzuki coupling procedure. Synthetic routes of pyrene-thiol derivative A-SH was presented in Scheme 1. As shown in Scheme 1, compound A-SH was obtained by a combination of Suzuki coupling procedure, nucleophilic substitution, etc. The pyrene-thiol derivative was evidenced by typical peaks at 480.0 m/z in the mass spectra. In addition, with the ^{1}H-NMR and FI-IR spectra, the final compound was fully characterized.

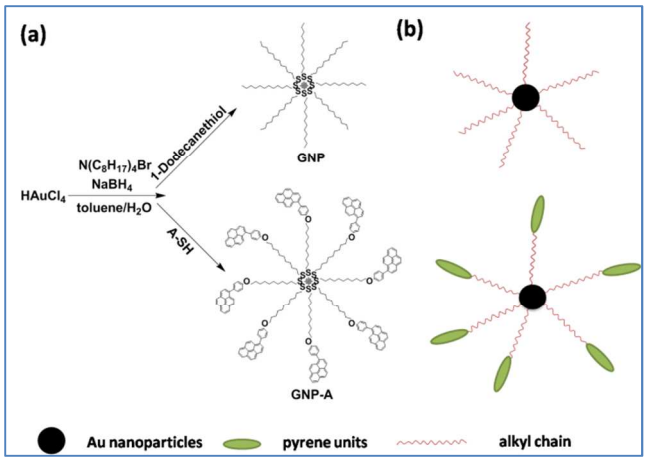

Scheme 2. Schematic representation of the functionalization of Au nanoparticles with 1-dodecanethiol and pyrene-thiol derivative **A-SH**.

Pyrene-thiol derivative A-SH and 1-dodecanethio were functionalized on Au nanoparticles by adopting a biphasic synthetic procedure similar to realize the morphology-control of nanoparticle by the capped side groups, which was shown in Scheme 2. Gold nanoparticles were functionalized with the corresponding thiol derivatives in molar ratio of 1:10 to obtain Au nanoparticles under 10 nm sizes. In the preparation of functionalized gold nanoparticles, an aqueous solution of hydrogen tetrachloroaurate (III) hydrate was stirred with tetraoctylammonium bromide, until all the aurate ions were transferred into the toluene layer. To this was added a solution of thiol derivatives and after stirring for several minutes, sodium borohydride was added to reduce the Au and the hybrid nanoparticles were obtained.

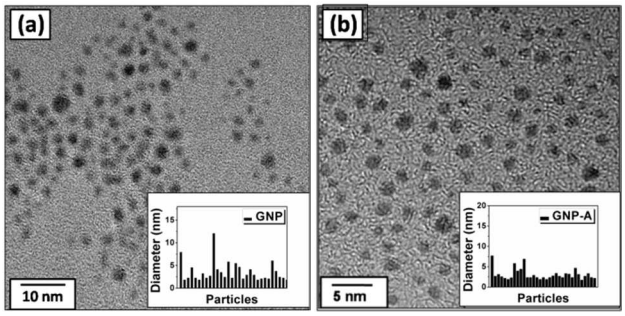

Figure 1. TEM images of gold nanoparticles functionalized with (a) 1-dodecanethiol (GNP) and (b) A-SH (GNP-A) after drop casting onto a carbon-coated copper grid. Insert shows the particle size distributions.

Various methods adopted for the characterization of monolayer-protected clusters of gold nanoparticles have been reviewed recently by Murray and co-workers.[3] In the present case, the pyrene-thiol-capped Au nanoparticles were characterized using High-Resolution Transmission Electron Microscopy (HRTEM). The HRTEM images of gold nanoparticles functionalized with 1-Dodecanethiol and A-SH is presented in Figure 1. Samples were prepared by drop casting the nanoparticles suspension onto a carbon-coated copper grid (for details, see the Experimental section). Images presented in Figure 1 indicated the presence that both 1-dodecanthiol functionalized Au nanoparticles (GNP) and A-SH functionalized Au nanoparticles (GNP-A) showed average sizes of 2.5 nm. There was lager clusters (> 3 nm) observed on the grid which might be formed as a result of the interparticle aggregation of smaller particles. Inserts of the images gave the particles size distributions of the samples.

UV-Vis and PL Spectra

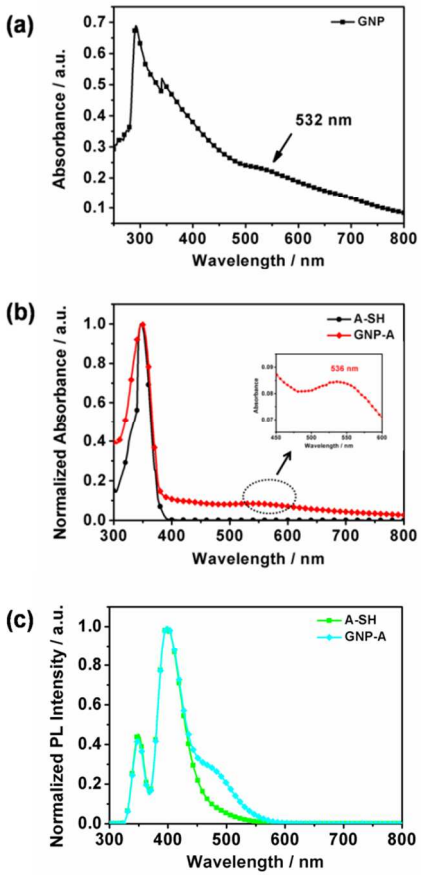

Figure 2. Absorption spectra of (a) Au nanoparticles functionalized by 1-dodecanethiol, (b) A-SH and Au nanoparticles functionalized by A-SH; Emission spectra of (c) A-SH and the Au nanoparticles functionalized by A-SH.

Absorption spectra of Au nanoparticles functionalized by 1-dodecanethiol (GNP) and pyrene-thiol-capped Au nanoparticles (GNP-A), as well as the emission spectra of GNP-A, were presented in Figure 2. Absorption spectrum of GNP given in Figure 2(a) possessed a broad band in the visible region as well as a typical structured absorption band at approximately 532 nm, which were all attributed to the surface plasmon absorption and the size of Au nanoparticles.[23] The surface plasmon absorption originated from the interaction of external electromagnetic radiation with highly polarizable Au $5d^{10}$ electrons of Au nanoparticles.[24]

The absorption characteristics of compound A-SH and the pyrene-thiol-capped nanoparticles GNP-A were shown in Figure 2(b). Pyrene-thiol derivative A-SH showed an obvious absorption band at 345 nm, which was a typical structured absorption band of pyrene chromophores. When functionalized on Au nanoparticles, the structured absorption band of pyrene chromophore remained unperturbed, and the structured absorption band of Au nanoparticles appeared at approximately 536 nm. Although surface capping by pyrene-thiol ligands did cause a small shift in the plasmon band maxima from that observed with GNP, the modified nanoparticles of GNP and GNP-A showed similar size and morphology (Figure 1). Indeed, the plasmon band energies of both series of functionalized nanoparticles were, for the most part, independent of the chemical identity of the appended ligand.[25]

The emission spectral properties of GNP-A gold nanoparticles and compound A-SH in CH_2Cl_2 solutions were compared in Figure 2(c). By comparing to A-SH, GNP-A nanoparticles exhibited a new shoulder peak at 485 nm, which was attributed to the excimer emission of pyrene chromophores. Excimer emission was usually observed in the spectral region of 425-600 nm when the concentration of pyrene core was high enough to form excited state dimmers or in constrained/heterogeneous media wherein the mobility of the polynuclear aromatic hydrocarbon molecules was minimized.[20] The concentration dependence of pyrene chromophore binding to Au nanoparticles was earlier investigated by Chen and Katz by titrating Au nanoparticles with pyrene chromophore possessing thiester / thicarbonate functional group.[26, 27]

Self-assembly properties

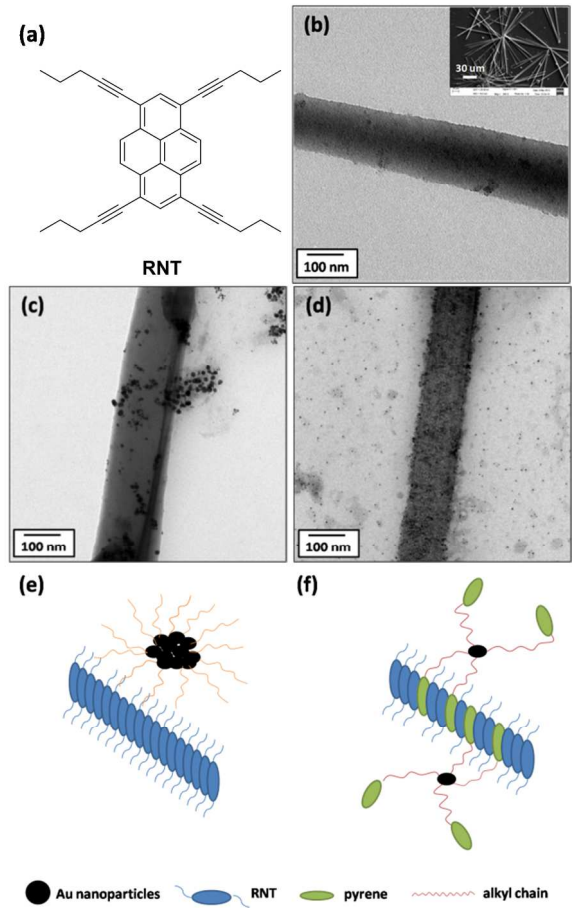

Figure 3. Self-assembly morphologies of pyrene derivative composited with gold nanoparticles. (a) molecular structure of pyrene derivative RNT; (b) TEM and SEM images of self-assembled RNT; (c) TEM image of self-assembled RNT composited with GNP nanoparticles; (d) TEM image of self-assembled RNT composited with GNP-A nanoparticles; (e) the possible arrangement of self-assembled RNT-GNP composite; (f) the possible arrangement of self-assembled RNT-GNP-A composite.

Figure 3(a) gave the molecular structures of pyrene derivatives 1,3,6,8-tetra(pent-1-yn-1-yl) pyrene (RNT) that we synthesized before, which showed well self-assembly behavior for the strong π-π interactions. By using solvent-exchange method in solution phase (for details, see the Experimental section), RNT molecules

could self-assembly into regular morphology as was shown in Figure 3(b). Rod-like structures of RNT molecules with ~100 nm in width could be observed by combined characterizations of SEM and TEM.

Figure 4 gave the PL spectroscopic titration experiment of RNT solutions with quantitative addition of GNP-A. In Figure 4, the fluorescence intensity of RNT in dichloromethane typically decreased with the addition of GNP-A, which may attribute to the π-π interactions between the pyrene rings of RNT and GNP-A in solutions. Co-assembly experiments of these RNT-NPs composites were carried out by separately mixing RNT with GNP and GNP-A in CH_2Cl_2 solutions. The conformational flexibility of the functional side groups of the Au nanoparticles gave them sufficient solubility in hydrophobic solvent of CH_2Cl_2 and equal amount of GNP and GNP-A was added into RNT solutions respectively. TEM images in Figure 3(c) and 3(d) showed the morphologies of self-assembled RNT-GNP and RNT-GNP-A composites. In Figure 3(c), RNT molecules self-assembled into rod-like structures and GNP nanoparticles were aggregated into nanocluster for the limited solubility in poor solvent of ethanol. However, in Figure 3(d) GNP-A nanoparticles uniformly dispersed and mostly arranged along the self-assembled RNT rods. By comparing the self-assembled morphologies of these two composites, it could be observed that GNP-A nanoparticles showed better dispersity in the solvent than GNP nanoparticles. More importantly, unlike GNP nanoparticles, GNP-A nanoparticles could have better interactions with RNT molecules and this may be attributed to the π-π interactions between the functional pyrene groups and the RNT molecules as were shown in Figure 3(e) and Figure 3(f). Thus, this method to form well co-assembly structures by modifying Au nanoparticles with functional groups we provided is applicable to a wide variety of NP systems and we expect that this will have potential for versatile applications in electronic and optical nanodevices.

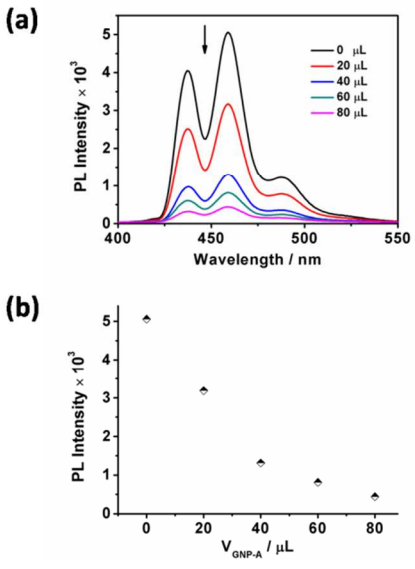

Figure 4. (a) Changes in the PL spectra of RNT in dichloromethane excited by 428 nm with the addition of quantitative 0.5 mg/mL GNP-A solution and (b) the different PL intensities of RNT at 459 nm during the PL spectroscopic titration experiment.

Conclusion

In summary, gold nanoparticles capped with 11-(4-(pyren-1-yl)phenoxy)undecane-1-thiol and with 1-dodecanethiol were prepared and characterized. The TEM images of these nanoparticles both showed similar particles size at approximately 2.5 nm as well as evidenced by the absorption spectra. By co-self-assembly of pyrene derivative composited with these functionalized nanoparticles, different morphologies of Au nanoparticles were observed by TEM. Comparing to Au nanoparticles functionalized by 1-dodecanethiol, pyrene-thiol-capped gold nanoparticles distributed well on the self-assembled nanostructures of pyrene derivative for the π-π interactions. This result reflected the artificial control of nanoparticles via versatile functionalities, which might represent a substantial advancement in small-scale device applications.

Experimental section

Materials

Reagents were purchased from commercial sources and used without further purification. Solvents were distilled in the standard methods and purged with argon before use.

Synthesis of S-(11-bromoundecyl) ethanethioate (1). 350 mg of AIBN (98% 2.15 mmol) was added to a solution of thioacetic acid (1.60 ml, 21.45 mmol) and 11-bromo-1-decene (1.00 g, 4.29 mmol) in toluene (45 ml). The mixture was stirred and heated at 95 °C for 4 h. Then, the volatiles were removed in vacuo. The resulting orange oil was dissolved in CH_2Cl_2 (100 ml) and washed with a saturated solution of NaCl (50 ml) and with a saturated solution of $NaHCO_3$ (50 ml). The organic phase was dried with anhydrous $MgSO_4$ and the solvent was removed under reduced pressure yielding a yellow solid. The product was purified by chromatography on a silica gel column with PE/CH_2Cl_2 (2:1) as eluent. The desired compound was obtained as bright yellow oil. Yield: 1.30 g (98%). ^{1}H-NMR (400 MHz, $CDCl_3$): δ = 3.42 (2H, m), 2.88 (2H, m), 2.34 (3H, s), 1.86 (2H, m), 1.59 (2H, m), 1.44 (2H, m), 1.36 (2H, m), 1.29 (2H, m) ppm. ^{13}C-NMR (100 MHz, CDCl3): δ = 194.9, 33.7, 32.6, 32.5, 30.5, 29.6, 29.3, 29.2, 28.7, 28.6, 28.0 ppm. FT-IR (KBr): 2926, 2854, 1694, 1463, 1353, 1251, 1134, 952, 722, 627 cm^{-1}. MALDI-TOF-MS (dithranol): m/z: calcd for $C_{13}H_{25}BrOS$: 308.08 g mol^{-1}, found: 309.3 g mol^{-1} $[MH]^+$. Elemental analysis calcd (%) for $C_{13}H_{25}BrOS$ (309.20): C 51.47, H 8.11, S 10.38; found: C 51.50, H 8.09, S 10.40.

Synthesis of 4-(pyren-1-yl)phenol (2).

1-bromopyrene (1.00 g, 3.58 mmol) was dissolved in 30 ml of anhydrous THF and the mixture was degassed via ultrasonic under nitrogen atmosphere for 45 min. Then, 4-Hydroxyphenylboronic acid (0.50 g, 3.58 mmol) and catalytic agents $Pd(PPh_3)_4$ (0.04 g, 0.03 mmol), K_3PO_4 (15.20 g, 71.60 mmol) were added and the reaction mixture was heated to 85 °C and stirred for 8 hours under nitrogen atmosphere. The cooled reaction mixture was diluted with CH_2Cl_2 and extracted with water. The organic phase was dried with $MgSO_4$ and the solvent was removed under reduced pressure. The crude product was purified by column chromatography (silica gel, dichloromethane / petroleum ether = 1 / 1, v / v) to give compound **2**. Yield: 0.95 g (90%). ^{1}H-NMR (400 MHz, $CDCl_3$): δ = 8.24 (3H, d, J = 6.8 Hz),

8.20 (1H, m), 8.13 (2H, d, J = 6.8 Hz), 8.06 (2H, d, J = 6.8 Hz), 7.99 (1H, d, J = 6.8 Hz), 7.56 (2H, d, J = 6.8 Hz), 7.06 (2H, d, J = 6.8 Hz) ppm. ^{13}C-NMR (100 MHz, $CDCl_3$): δ = 157.4, 134.6, 133.9, 133.3, 132.2, 130.5, 128.8, 128.3, 126.6, 126.3, 125.6, 125.1, 123.3, 121.9, 116.4, 115.5 ppm. FT-IR (KBr): 3789, 1593, 1471, 1229, 835, 753, 504 cm^{-1}. MALDI-TOF-MS (dithranol): m/z: calcd for $C_{22}H_{14}O$: 294.10 g mol^{-1}, found: 294.3 g mol^{-1} $[MH]^+$. Elemental analysis calcd (%) for $C_{22}H_{14}O$ (294.10): C 89.76, H 4.76; found: C 89.79, H 4.77.

Synthesis of S-(11-(4-(pyren-1-yl)phenoxy)undecyl) ethanethioate (3).

Compound 2 (0.50 g, 1.70 mmol) and K_2CO_3 (0.71 g, 5.10 mmol) were added to a solvent of DMF (50 ml) and the mixture was stirred under nitrogen atmosphere for 1 hour. Then compound 1 (1.57 g, 5.10 mmol) was added and the reaction mixture was heated to 100 ^{o}C and reacted for 24 hours. The cooled reaction mixture was diluted with CH_2Cl_2 and extracted with water. The organic phase was dried with $MgSO_4$ and the solvent was removed under reduced pressure. The crude product was purified by column chromatography (silica gel, dichloromethane / petroleum ether = 1 / 3, v / v) to give compound **3**. Yield: 0.71 g (80%). ^{1}H-NMR (400 MHz, $CDCl_3$): δ = 8.24 (3H, d, J = 6.8 Hz), 8.20 (1H, m), 8.12 (2H, d, J = 6.8 Hz), 8.06 (2H, d, J = 6.8 Hz), 7.99 (1H, d, J = 6.8 Hz), 7.58 (2H, d, J = 6.8 Hz), 7.12 (2H, d, J = 6.8 Hz), 4.11 (2H, m), 2.90 (2H, m), 2.35 (3H, s), 1.90 (2H, m), 1.60 (16H, m) ppm. ^{13}C-NMR (100 MHz, $CDCl_3$): δ = 194.9, 158.3, 133.9, 133.6, 133.3, 132.2, 129.7, 128.8, 128.3, 126.6, 126.3, 125.6, 125.1, 123.3, 121.9, 115.5, 114.9, 68.7, 32.5, 30.5, 29.6, 29.3, 29.2, 28.7, 25.9 ppm. FT-IR (KBr): 2923, 2851, 1688, 1606, 1498, 1243, 836 cm^{-1}. MALDI-TOF-MS (dithranol): m/z: calcd for $C_{35}H_{38}O_2S$: 522.26 g mol^{-1}, found: 522.7 g mol^{-1} $[MH]^+$. Elemental analysis calcd (%) for $C_{35}H_{38}O_2S$ (522.26): C 80.42, H 7.33, S 6.13; found: C 80.44, H 7.32, S 6.12.

Synthesis of 11-(4-(pyren-1-yl)phenoxy)undecane-1-thiol (A-SH).

1.15 ml of concentrated HCl (37%, 13.94 mmol) were added to a solution of **3** (0.56 g, 1.08 mmol) in MeOH (20 ml). The mixture was heated to reflux for 3 hours. After this time 30 ml of water were added and the resulting solution was extracted with diethyl ether (3×30 ml). The organic phase was dried with anhydrous $MgSO_4$ and the solvent was evaporated at reduced pressure yielding **A-SH**. Yield: 0.39 g (75%). ^{1}H-NMR (400 MHz, $CDCl_3$): δ = 8.24 (3H, d, J = 6.8 Hz), 8.20 (1H, m), 8.12 (2H, d, J = 6.8 Hz), 8.06 (2H, d, J = 6.8 Hz), 7.99 (1H, d, J = 6.8 Hz), 7.58 (2H, d, J = 6.8 Hz), 7.12 (2H, d, J = 6.8 Hz), 4.11 (2H, m), 2.58 (2H, m), 1.90 (2H, m), 1.60 (13H, m), 0.90 (4H, m) ppm. ^{13}C-NMR (100 MHz, $CDCl_3$): δ = 158.3, 133.9, 133.6, 133.3, 132.2, 129.7, 128.8, 128.3, 126.6, 126.3, 125.6, 125.1, 123.3, 121.9, 115.5, 114.9, 68.7, 34.2, 29.6, 28.9, 28.2, 25.9, 24.6 ppm. FT-IR (KBr): 2921, 2852, 1605, 1467, 1245, 1111, 844, 756 cm^{-1}. MALDI-TOF-MS (dithranol): m/z: calcd for $C_{33}H_{36}OS$: 480.25 g mol^{-1}, found: 480.7 g mol^{-1} $[MH]^+$. Elemental analysis calcd (%) for $C_{33}H_{36}OS$ (480.25): C 82.45, H 7.55, S 6.67; found: C 82.46, H 7.57, S 6.65.

Function of gold nanoparticles

Sized gold clusters capped with 1-dodecanethiol and pyrene-thiol A-SH were synthesized according to the Brust procedure.[12] In the preparation of A-SH functionalized gold nanoparticles, an aqueous solution of hydrogen tetrachloroaurate (III) hydrate (50 μmol in 2 mL) was stirred with tetraoctylammonium bromide (250 μmol in 5 ml of toluene) for 5 min, until all the aurate ions were transferred into the toluene layer. To this was added a solution of A-SH, in the molar ratio 1:10 in 2 ml of toluene. After stirring for 2-3 min, sodium borohydride (2.5 mmol in 2 ml of water) was added and the mixture was stirred for 3 h. The hybrid nanoparticles formed were purified by repeated precipitation and filtration using ethanol (3×100 ml). The brown powder obtained was redispersed in toluene.

Preparations of the TEM grid

For the characterization of Au nanoparticless by TEM, a carbon-supported copper grid (Okenshoji, Model: STEM100 Cu grid) was used. The grid was stored in a desiccator and used without any treatment. An ethanol-toluene solution containing Au nanoparticles was aged for more than 2 days and dropped (0.05 ml) onto the grid. All grids were dried naturally for 1 day before the TEM observation.

Self-assembly of gold nanoparticles and discotic molecules

Self-assembly of the RNT and the RNT-GNP composites was conducted by using the solvent-exchange method in the solution phase, which transfers the molecules from a good solvent (CH_2Cl_2) into a poor solvent (ethanol) where the molecules have limited solubility, and thus self-assembly occurs through π-π stacking. This approach takes the advantage of the strong intermolecular π-π interactions, which are enhanced in a poor solvent where the molecules have minimum interaction with the solvent. Similar methods have previously been used for self-assembling 1D nano- or microstructures of π-conjugated organic molecules.[28-30] In our experiments, we used a solution-injection method to facilitate the self-assembly in the ethanol medium. Typically, a minimum volume (50 μl) of a concentrated CH_2Cl_2 solution (0.001 M) of RNT was injected rapidly into a larger volume (5 ml) of ethanol, followed by immediate mixing. Thus, the mixed solution contained only a slight amount of toluene, resulting in the effective self-assembly of the molecule. Such a solvent provided limited solubility for RNT molecules, but on the other hand leaded to favorable molecular π-π stacking.

Characterization

^{1}H-NMR spectra of the samples were recorded with a Varian 400 MHz instrument. All UV-visible spectra were recorded on a HITACHI U-3010 spectrophotometer, and all fluorescence spectra were recorded on a HITACHI F-4500 fluorescence spectrophotometer. FT-IR spectroscopy was recorded on a Perkin Elmer LR-64912C spectrophotometer. MALDI-TOF-MS spectra were determined on a Shimadzu AXIMA-CFR mass spectrometer. SEM observation was performed with a Jeol JSM-5400/LV. The accelerating voltage was 15 kV. TEM images were obtained by using transmission electron microscopy (H7100, Hitachi, 100 kV).

Acknowledgements

This work was supported by the National Natural Science Foundation of China (Grant No.51173017, 51373024, 51203011, 51103010, and 61370048), the Major Project of International

Cooperation of the Ministry of Science and Technology (Grant No. 2013DFB50340), the Major Project of Beijing Science and Technology Program (Grant No. Z121100006512002) and Beijing Natural Science Foundation (2122042).

Notes and references

[a] *Department of Materials Physics and Chemistry, School of Materials Science and Engineering, University of Science and Technology Beijing, Beijing 100083, People's Republic of China. Fax: +86-10-62333759; Tel: +86-10-62333759; E-mail: yangz@ustb.edu.cn; wangdong_ustb@foxmail.com*

[b] *Department of Materials Science and Engineering, College of Engineering, Peking University, Beijing 100871, People's Republic of China. E-mail: yanghuai@pku.edu.cn*

1 P. V. Kamat, *J. Phys. Chem. B,* 2002, **106**, 7729.
2 I. I. Binil, K. T. George, *J. Phys. Chem. B,* 2004, **108**, 13265.
3 A. C. Templeton, W. P. Wuelfing, R. W. Murray, *Acc. Chem. Res.,* 2000, **33**, 27.
4 H. Imahori, S. Fukuzumi, *Adv. Mater.,* 2001, **13**, 1197.
5 R. Shenhar, V. M. Rotello, *Acc. Chem. Res.,* 2003, **36**, 549.
6 M. Sastry, M. Rao, K. N. Ganesh, *Acc. Chem. Res.,* 2002, **35**, 847.
7 K. G. Thomas, P. V. Kamat, *Acc. Chem. Res.,* 2003, **36**, 888.
8 H. Imahori, H. Norieda, H. Yamada, Y. Nishimura, I. Yamazaki, Y. Sakata, S. Fukuzumi, *J. Am. Chem. Soc.,* 2001, **123**, 100.
9 V. Berry, R. F. Saraf, *Angew. Chem., Int. Ed.,* 2005, **44**, 6668.
10 (a) A. Imre, G. Csaba, L. Ji, A. Orlov, G. H. Bernstein, W. W. Porod, *Science,* 2006, **311**, 205; (b) S. A. Maier, P. G. Kik, H. A. Atwater, S. Meltzer, E. Harel, B. E. Koel, A. A. G. Requicha, *Nat. Mater.* 2003, **2**, 229.
11 (a) S. Zhongrong, Y. Mami, M. Mikio, *J. Am. Chem. Soc.,* 2007, **129**, 14271; (b) R. P. Cowburn, M. E. Welland, *Science,* 2000, **287**, 1466.
12 M. Brust, M. Walker, D. Betheli, D. J. Schiffrin, R. Whyman, *J. Chem. Soc.,* 1994, **80**.
13 W. Tongxin, Z. Deping, X. Wei, Y. Junlin, H. Rui, Z. Daoben, *Langmuir,* 2002, **18**, 1840.
14 A. Laromaine, L. Koh, M. Murugesan, R. V. Ulijn, M. M. Stevens, *J. Am. Chem. Soc.,* 2007, **129**, 4156.
15 J. Jin, T. Iyoda, C. Cao, Y. Song, L. Jiang, T. Li, D. Zhu, *Angew. Chem., Int. Ed.,* 2001, **40**, 2135.
16 T. Wang, D. Zhang, W. Xu, J. Yang, R. Han, D. Zhu, *Langmuir,* 2002, **18**, 1840.
17 R. G. Nirmal, A. L. Kavitha, S. Berchmans, V. Yegnaraman, *J. Nanosci. Nanotechnol.,* 2007, **7**, 2116.
18 H. Ozawa, M. Kawao, H. Tanaka, T. Ogawa, *Langmuir,* 2007, **23**, 6365.
19 K. Kalyanasundaram, Photochemistry in Microheterogeneous Systems, *Academic PressInc.: Florida,* 1987.
20 J. B. Bricks, Photophysics of Aromatic Molecules; *Wiley: London*, 1970.
21 K. Yuko, K. Takashi, *Org. Lett.,* 2006, **8**, 2463.
22 (a) S. Perumal, A. Hofman, N. Scholz, E. Ruhl, C. Graf, *Langmuir*, 2011, **27**, 4456; (b) D. S. Karpovich, G. J. Blanchard, *Langmuir,* 1996, **12**, 5522.
23 C. Marina, A. F. Marye, K. W. James, *Photochem. Photobiol. Sci.*, 2003, **2**, 1177.
24 M. M. Alvarez, J. T. Khoury, T. G. Schaaff, M. N. Shafigullin, I. Vezmar, R. L. Whetten, *J. Phys. Chem. B,* 1997, **101**, 3706.
25 U. Kreibig and M. Vollmer, *Springer Ser. Mat. Sci*., 1995, **25**.
26 M. M. Y. Chen, A. Katz, *Langmuir,* 2002, **18**, 2413.
27 M. M. Y. Chen, A. Katz, *Langmuir,* 2002, **18**, 8566.
28 J. E. Anthony, J. S. Brooks, D. L. Eaton, S. R. Parkin, *J. Am. Chem. Soc.,* 2001, **123**, 9482.
29 J. E. Anthony, D. L. Eaton, S. R. Parkin, *Org. Lett.,* 2002, **4**, 15.
30 H. K. Do, Y. L. Dong, S. L. Hwa, H. L. Wi, H. K. Yong, I. H. Jeong, C. Kilwon, *Adv. Mater.,* 2007, **19**, 678.
31